Int J Cardiovasc Imaging
DOI 10.1007/s10554-009-9529-z

ORIGINAL PAPER

New X-ray imaging modalities and their integration with intravascular imaging and interventions

H. Hetterich · T. Redel · G. Lauritsch · C. Rohkohl · J. Rieber

Received: 4 February 2009 / Accepted: 22 October 2009

Abstract During recent years various techniques emerged providing more detailed images and insights in the cardiovascular system. C-Arm computed tomography is currently introduced in cardiac imaging offering the potential of three dimensional imaging of the coronary arteries, the cardiac chambers, venous system and a variety of anatomic anomalies inside the interventional environment. Furthermore it might enable perfusion imaging during percutaneous coronary intervention (PCI). Intravascular ultrasound (IVUS) and optical coherence tomography (OCT) are meanwhile established tools for detailed assessment of the coronary arteries. Their use might further increase with automated tissue characterization, three dimensional reconstruction, integration in angiography systems, and new emerging techniques. Parameters of fluid tissue interactions are important factors in the pathogenesis of atherosclerosis. These parameters can be calculated using computational fluid dynamics based on three dimensional models of the coronary vessels which can be derived from various sources including mulitslice computed tomography (MSCT), C-Arm CT or 3D reconstructed IVUS or OCT. Their use in the clinical setting has yet to be determined especially with regard to their ability in increasing treatment efficiency and clinical outcome.

Keywords C-Arm computed tomography · Intravascular ultrasound · Optical coherence tomography · Computational fluid dynamics

Introduction

Cardiovascular disease remains a leading cause of morbidity and mortality among the developed countries and is also becoming increasingly important in the emerging countries [1–4]. During the last decades various different disease entities have been discovered and for many of them also treatment options have been proposed. Further miniaturization of the devices has led to a trend towards less invasive therapies for coronary artery disease, valvular heart disease, congenital anomalies and cardiac arrhythmias [5–10]. Accurate imaging modalities are of paramount importance for the guidance of these complex interventional procedures in the cath lab. Depending on the procedure different types of information are desired ranging

H. Hetterich · J. Rieber (✉)
Department of Cardiology, Medizinische Poliklinik, University of Munich, Ziemssenstr. 1, 80336 Munich, Germany
e-mail: Johannes.Rieber@med.uni-muenchen.de

T. Redel · G. Lauritsch · C. Rohkohl · J. Rieber
Siemens AG, Healthcare Sector, Siemensstr. 1, 91301 Forchheim, Germany

C. Rohkohl
Chair of Pattern Recognition, Department of Computer Science, Friedrich-Alexander University Erlangen-Nuremberg, Martensstr. 3, 91058 Erlangen, Germany

Published online: 08 November 2009

from an overview of the gross vascular anatomy to submilimeter structures and functional parameters. These different problems require a variety of imaging modalities in the interventionalist's armamentarium. The aim of this paper is to give an overview about some available and emerging techniques and provide a glimpse into the future for potential new developments and applications.

C-Arm computed tomography (C-Arm CT)

Angiography is considered the standard of reference for imaging and guiding of cardiovascular interventions. It is a technique that is relatively easy to perform and provides an overview of the vascular system with an unsurpassed spatial and temporal resolution [11].

Traditionally angiography was performed using monoplane or biplane system, consisting of a radiation source and a detector. With the improvement in detector technology these systems can today not only be used for two dimensional (2D) display but can also acquire three dimensional (3D) data similar to multislice computed tomography (MSCT) [12–17]. The common principle is that the tube and the detector are rotating around the patient, e.g. over 200°. Several hundred images are acquired depending on the specific protocol. The 2D raw projection data is used to reconstruct 3D volume data sets using a 3D cone-beam reconstruction algorithm [6, 18]. Subsequently the data can be displayed as either tomographic images or as 3D models. This approach is called C-Arm computed tomography (C-Arm CT). The technique requires state-of-the-art C-Arm systems equipped with flat panel detectors. To achieve C-Arm CT results with good low-contrast visibility, sophisticated correction techniques are needed including correction for overexposure, scatter, beam-hardening, truncation and ring artifacts [19].

For imaging of the heart the C-Arm system performs multiple runs around the patient while the electrocardiogram (ECG) is monitored. For better enhancement a continous injection of contrast dye is necessary. Using retrospective ECG gating the raw data can be reconstructed for a particular phase of the cardiac cycle [6]. The main advantage of these systems is their availability during interventions in the cath lab without any patient transfer.

One application is the treatment of atrial fibrillation. The disease affects a large number of patients and although it is per se benign can lead to variety of complications and significantly reduces the patient's quality of life [20]. In certain cases the origin of the disease can be located in the area of the orifice of the pulmonary veins. In these cases atrial fibrillation can be treated by isolating the pulmonary veins from the atrium by catheter ablation. Such procedures may take several hours and are often associated with fluoroscopy times of 60 min and more [21–23]. Exact imaging might help to reduce procedure time, radiation exposure and complication rates especially when available during the procedure. Using the 3D information provided by C-Arm CT the relevant parts of the cardiac geometry can be segmented and an overlay can be created to guide the intervention (Fig. 1). Furthermore C-Arm CT can display surrounding structures and therefore prevent and detect complications like esophageal fistulas which is a typical complication during pulmonary vein isolation [24, 25].

Another example where an optimal 3D orientation is extremely helpful are cases of congenital anomalies.

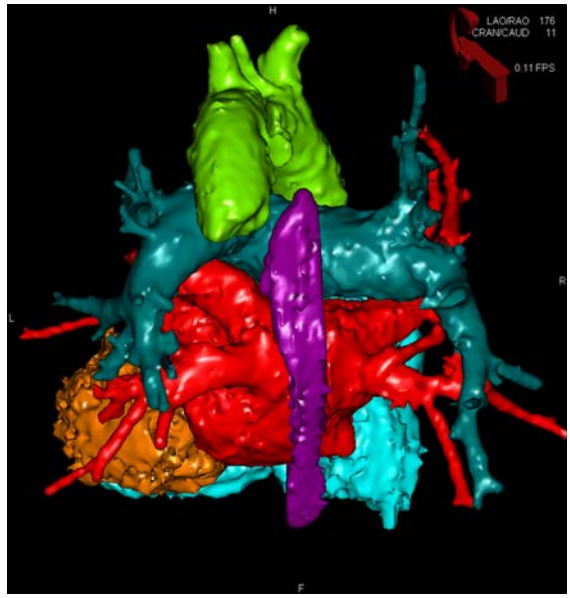

Fig. 1 Visualization of the segmented cardiac chambers and large thoracic vessels by C-Arm CT. The left atrium and the pulmonary veins (*red*), the left ventricle (*orange*), the aorta (*green*), the right atrium and ventricle (*light blue*), the pulmonary arteries (*dark blue*) and the esophagus (*purple*) can clearly be identified. (By courtesy of Prof. J. Brachmann, Coburg Hospital, Germany)

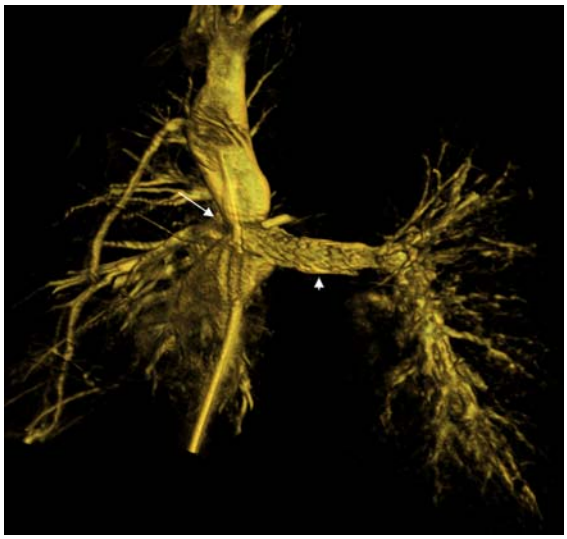

Fig. 2 Example of a 5-year old patient with hypoplastic left heart syndrome. The patient underwent palliative surgery with a cavopulmonary anastomosis and placement of a stent in the pulmonary artery. C-Arm CT was performed for evaluation before Fontan surgery. The pulmonary vasculature, the cavopulmonary anastomosis (*arrow*) and the patent stent within the pumonary artery (*arrowhead*) were clearly displayed. Radiation exposure was less compared to conventional CT imaging. (By courtesy of Dr. P. Ewert; German Heart Institute, Berlin)

Fig. 3 Motion compensated 3D reconstruction of the left coronary artery obtained by C-Arm CT. The picture shows the coronary catheter (*A*), the left main (*B*), the left anterior descending (*C*) and the left circumflex artery (*D*)

Beyond open surgical approaches the optimal treatment also frequently comprises interventional techniques such as dilation of stenosis of the great arteries or closure of shunts [8, 9]. Since C-Arm CT is capable of providing high quality 3D imaging in complex cases with usually lower radiation doses than conventional CT [19] this technique is more and more applied also in pediatric cardiology (Fig. 2).

Since the rotation speed of the C-Arm is significantly slower than in traditional CT, this causes problems if a visualization of moving structures is desirable. In this case an automated motion correction has to be applied. Motion is estimated by 3D/3D registration of a set of preliminary 3D volume images of different cardiac phases reconstructed from a sparse subset of ECG gated projection data. For the final reconstruction the complete projection data is used. The motion in the data is compensated by a deformed backprojection step along curved lines according to the precalculated motion vector field [26, 27].

An especially interesting application of this technique is the 3D imaging of the coronary artery tree by intracoronary injection of contrast dye similar to a 2D conventional coronary angiography (Fig. 3). A 3D representation of the coronary anatomy may be desired for percutaneous coronary interventions (PCI) in complex cases like stenosis of the left main coronary artery or branching points.

Furthermore visualization of the coronary veins is important in some patients suffering from heart failure. Besides optimal medical treatment some patients benefit from cardiac resynchronization therapy by reestablishing a synchronous contraction of the left ventricular septum and free wall [28–31]. In addition to the right atrial and right ventricular lead a third lead, which is introduced in the coronary sinus for stimulation of the left ventricular free wall is used. The placement of this lead is often difficult and time consuming [31, 32]. Innovative approaches for mitral valve regurgitation repair may also rely on detailed information of the coronary sinus (CS) [33, 34]. An exact 3D reconstruction of the CS, which can be obtained by C-Arm CT might facilitate these procedures. By retrograde injection contrast dye is brought into the venous system via the CS using a

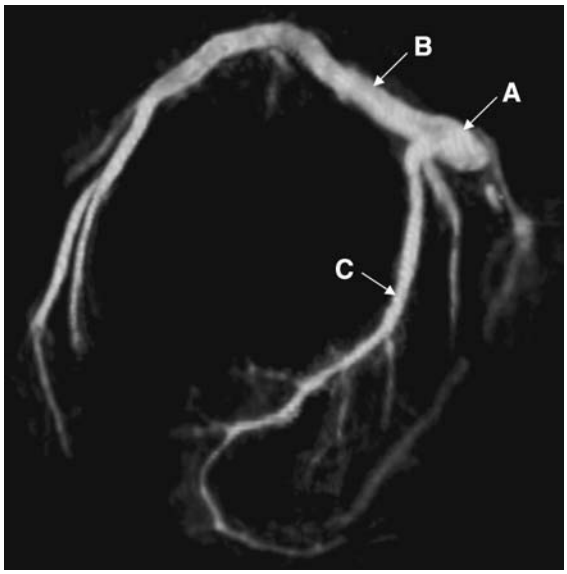

Fig. 4 Motion compensated reconstruction of the coronary venous system obtained by C-Arm CT. The picture was acquired after retrograde injection of contrast dye via a special catheter into the coronary sinus (*A*). Besides the coronary sinus the great cardiac vein (*B*) and the posterior vein of the left ventricle are displayed (*C*)

special blocking catheter to prevent a fast drain of the contrast dye [31] (Fig. 4).

Beyond the cardiac morphology also information about physiological parameters is desired. One vital example is the perfusion and vitality of the myocardium itself. This information can be used to detect myocardial ischemia or scarring. Traditionally photon emission tomography or magnetic resonance imaging is performed for that purpose [35, 36]. Newer studies indicate also a potential role for MSCT in perfusion analysis [37–39]. However, all these modalities are not available in the catheterization laboratory during PCI when this information is mostly desired for decision making. First images show that C-Arm CT might have the potential to aid in the assessment of perfusion as well and therefore further improve the workflow (Fig. 5).

Intravascular ultrasound (IVUS)

An intravascular ultrasound (IVUS) examination is performed during a cardiac catheterization procedure. By using a miniaturized ultrasound transducer mounted on a specially designed coronary catheter, cross-sectional images of the vessel can be obtained. IVUS uses a frequency spectrum of about 20–50 MHz to generate images with a axial and lateral resolution of about 150 –250 μm, respectively [40].

This technique allows a detailed assessment of the coronary vessel wall and geometry with a low intra and interobserver variability [41, 42]. IVUS is capable of visualizing non stenotic lesions undergoing positive remodeling which are often not recognized by coronary angiography but are frequently associated with plaque rupture leading to coronary

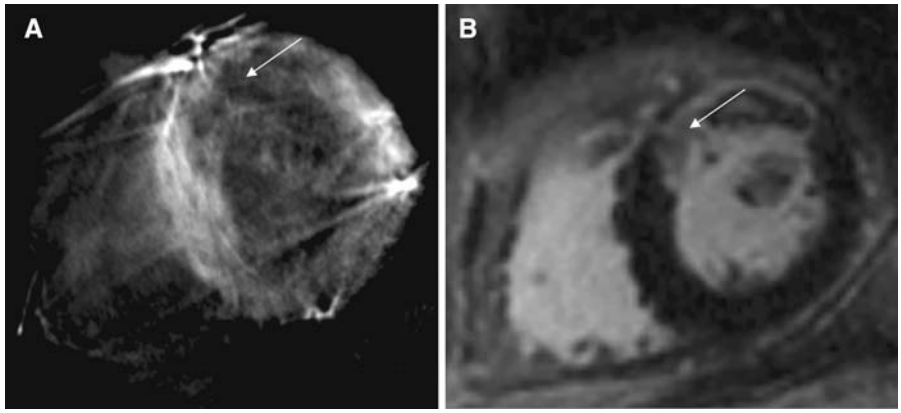

Fig. 5 Cross-sectional short axis of the left ventricle obtained by C-Arm CT (**a**) and magnetic resonance imaging (**b**). During first pass myocardial perfusion following intracoronary contrast injection into the left coronary artery, the C-Arm CT shows clearly a hypoperfusion of the left anterior wall (*arrow*). The MRI (*T1 weighted sequence*) revealed an area of late contrast enhancement of the respective area (*arrow*) indicating myocardial scar tissue. (By courtesy of Dr. H. Rittger and Dr. A. Sinha, Coburg Hospital, Germany)

thrombosis and myocardial infarction [43–47]. Furthermore IVUS is capable of assessing plaque burden and composition and is often used in clinical studies as a reference standard [48–51]. Nevertheless IVUS suffers from a couple of limitations especially in the identification of lipid rich plaques [51].

A reflected ultrasound signal consists of waves of different amplitude and frequency depending on the tissue where it has been reflected. Gray-scale IVUS only uses the information of signal amplitude. Radiofrequency data analysis (RF) also uses the information of the frequency spectrum for tissue characterization. Different parameters and different mathematical approaches have been used for RF [52–54]. Currently Virtual Histology^{TM} (VH), a commercially available software tool uses eight different spectral parameters. In VH four different plaque types are defined: fibrous, fibro-fatty, calcium, necrotic. Each plaque type is assigned a different color and the image is overlaid the gray scale image (Fig. 6) [55]. Nair et al. [56] showed that VH is able to differentiate between the various plaque components with accuracy between 89.5 and 92.8% depending on the plaque type. Using VH, vulnerable plaques are more often found in patients presenting with acute coronary syndrome, then in patients with stable angina [57]. RF thus might contribute to more sophisticated diagnosis and therapy of atherosclerotic coronary lesions. Current objectives for technical development include improvements of automation of signal processing and characterization of more tissue components.

IVUS as well as other modern invasive imaging techniques has a very high spatial resolution but almost no spatial orientation is provided. To estimate the position of the actual image, certain anatomic landmarks like sidebranches or bifurcations have to be used. Alternatively, angiography has to be performed during acquisition of the IVUS pullback to identify the position of the IVUS probe. Since the tissue information as provided by IVUS might have an increasing role for future interventional strategies, exact co-registration with other modalities such as angiography is desired. To achieve this goal several approaches have been investigated. One of these is the combination if the IVUS probe with a magnetic positioning system. The principle of the system is a magnetic array mounted on the table or the angiography system which generates a magnetic field. The positioning sensor can be miniaturized and coupled with the IVUS transducer. These systems yield submilimeter accuracy. Since these systems are operating using magnetic fields, no additional radiation is necessary. In fact, a reduction of the radiation burden is possible, since the positioning of the IVUS probe could be performed with less fluoroscopy. The disadvantage beyond the costs is the need for a designated magnetic array which can hamper the flexibility of the system.

Another step towards workflow improvement is image based co-registration. Here IVUS and angiographic data of a coronary segment are acquired and then matched using registration techniques. By this

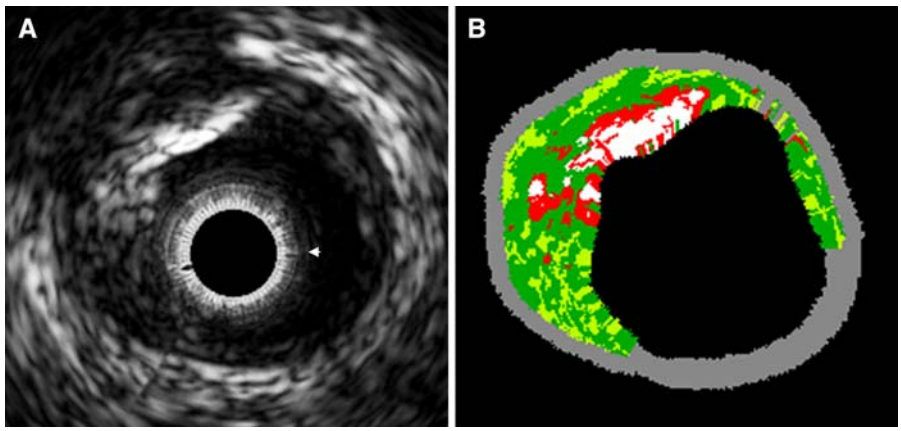

Fig. 6 IVUS and corresponding RF analysis image of a large atherosclerotic plaque. In the center is the catheter artifact (*arrow head*). *Gray scale* IVUS image (**a**) and color encoded RF analysis (**b**) show a large plaque with necrotic (*red*), calcified (*white*), fibro-lipidic (*light green*), fibrous (*dark green*) regions

the position and information of the IVUS catheter is linked to the angiographic information either in 2D or in 3D. Since IVUS is getting more and more important many of the cath labs have nowadays already integrated the IVUS imaging system into the angiography suite. Due to the combined use of IVUS and angiography as well as other imaging methods an additional benefit is achieved, which will most likely further increase the utilization of these new technologies.

Optical coherence tomography (OCT)

Optical coherence tomography (OCT) is a technique providing high resolution cross sectional images of biologic tissues [58–60]. Unlike IVUS, OCT uses light instead of ultrasound. The light beam is sent into the vessel wall and is then backscattered from different structures. Due to the high speed of light, it is not possible to measure the time-of-flight delay of the optical echoes for depth information directly. Therefore OCT uses the principles of interference and coherence for spatial resolution. The backscattered light from the tissue sample is superimposed to a light beam with a known reference path. Positive interference and therefore registration of the signal can only occur, if both pathways have exactly the same length, with an accuracy of the coherence length of the light used [58]. The main advantage of OCT is the superior resolution of 5–30 μm compared to other imaging techniques [58, 61]. For the use in coronary arteries a dedicated imaging catheter must be introduced into the vessels. Due to the different refractivity of blood plasma and cells a detailed assessment of the vessel wall in the presence of blood is not possible. A special occlusion catheter or high flow saline flushing has to be used to clean the artery from blood. Therefore imaging time is restricted to about 30 s [62, 63].

The first OCT systems used a rotating mirror to change the length of the reference pathway for the depth scan (time domain OCT). Unfortunately this was associated with a low imaging acquisition speed which precluded fast complete scans of the entire vessel. Newer systems which are currently evaluated in clinical trials are based on Fourier domain OCT which allows high speed imaging of long vessel segments within a few seconds during saline flushing without occlusion of the vessel. In Fourier domain OCT the depth information is gathered by dispersing different frequencies onto a detector. Through this the information of the depth scan can be obtained within a single light exposure. Another approach is swept source OCT. This technique uses a tunable laser source that rapidly sweeps its wavelength over the bandwidth. Due to the Fourier relation the depth scan can be immediately calculated by a Fourier-transform from the acquired spectra, without movement of the reference arm. Hereby imaging speed can be dramatically improved [64–68].

OCT provides a clear and detailed visualization of the vascular layers including the internal and external elastic membrane (Fig. 7) [69, 70]. It is also able to differentiate between different plaque components like fibrous, lipid rich and calcified tissue with high accuracy [63, 71–73]. OCT is the only imaging modality which allows the direct visualization of the thin fibrous cap of vulnerable plaques [62, 70, 74]. In post mortem study OCT was able to quantify the macrophage content of atherosclerotic lesions [75]. Therefore, OCT is the only technique capable of imaging all major features of high risk vulnerable plaques [76]. A drawback is the limited penetration depth of 1–2 mm, which is not sufficient to visualize large atheromas completely [77].

Since the introduction of drug eluting stents neointimal coverage of stent struts is a major concern. OCT is able to measure the thickness of coverage on sirolimus eluting stent struts [78]. It has shown to be able to detect balloon-induced dissection, intraluminal thrombus, cuts made by cutting ballons, tissue prolpse and suboptimally deployed stents (Fig. 7) [79]. OCT outperformes IVUS in the detection of dissection, tissue prolapse and incomplete stent deployment [80].

As mentioned earlier OCT is able to measure the macrophage density of atherosclerotic lesions [75]. Furthermore it is also possible to assess the collagen fiber content [81]. Therefore an automated tissue characterization as available for IVUS seems feasible. This technique may either be based on analysis of the frequency pattern as in VH or may use the texture information of the acquired images [82]. Due to its unique resolution OCT might be capable of extracting more features of atherosclerotic plaques allowing for a more precise plaque characterization then IVUS based techniques.

Agents offering high optical absorption or scattering can be used for positive or negative contrast

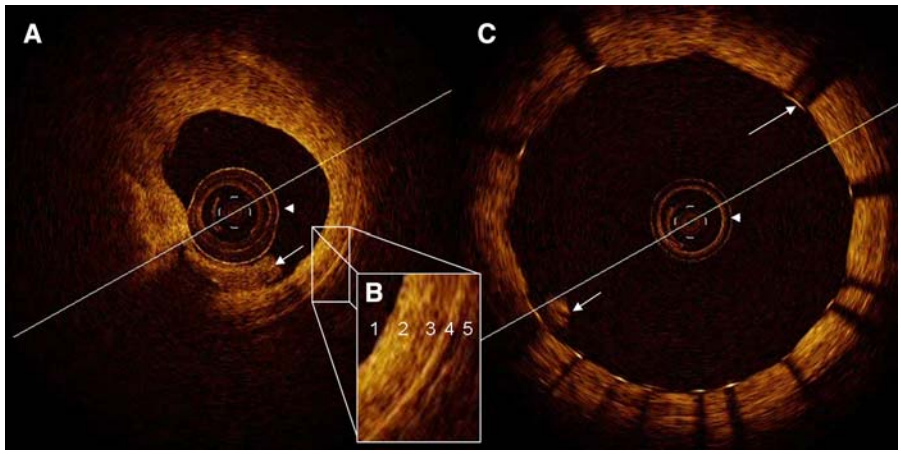

Fig. 7 OCT images of a left circumflex coronary artery before (**a, b**) and after stent implantation (**c**). In the center the artifact caused by the OCT imaging catheter can be seen (*arrow head*). Before treatment a large thrombus is visualized (**a**, *short arrow*). After the implantation the gain of lumen and the stent struts with dorsal shadowing (**c**, *long arrow*) are clearly displayed. Also a small protrusion of the thrombotic material is observed (C, *short arrow*). **b** Shows a magnification of the vessel wall with dark lumen (*1*) bright intimal thickening (*2*), dark media (*3*), bright external elastic membrane (*4*) and dark adventitia (*5*)

enhancement in OCT. Contrast agents which are currently developed include single molecules, nanoparticles and microspheres [83]. For the identification of atherosclerotic plaques agents indicating inflammation by phagocytosis of activated macrophages are of special interest [84].

Doppler wires are commonly used tools for the assessment of intracoronary flow characteristics and for determining the hemodynamic significance of intermediate stenosis. Like ultrasound, light reflected by a moving particle is Doppler shifted. Thus the direction and velocity of blood flow can be assessed. That way information about the anatomy and function of stenotic sites could be gathered with one examination [66].

Computational fluid dynamics calculations (CFD)

Most of the techniques described above offer detailed images of the coronary morphology but do not take into account physiologic and functional parameters and the interaction of the blood flow and vessel wall. Pathology studies revealed that atherosclerotic lesions are not randomly distributed within the vessel but show a preferred location at branches or bends. Therefore besides well known systemic risk factors local factors have to be taken into account. The complex vessel geometry disturbs the laminar flow and results in locally different shear stress levels which can promote atherosclerosis. In vitro research revealed a close correlation of endothelial shear stress and the natural history of atherosclerosis and vascular remodelling [85–87]. The parameters of flow-tissue-interaction namely Wall shear stress (WSS) are very difficult to measure directly in vivo. Nevertheless they can be calculated using computational fluid dynamics (CFD) if a 3D geometric model of the vessel is available [88–91]. The geometry information can be derived from various sources including MSCT, C-Arm CT or 3D reconstructed IVUS or OCT. The technique of CFD might lead to a more thorough understanding of plaque progression and might help to identify the vulnerability of a certain lesion. Furthermore stent implantations could be simulated before implantation to achieve optimal hemodynamic results [92, 93]. Initial in vivo studies show that very low as well as high shear stress levels are both associated with a higher prevalence of plaque and a higher average plaque thickness than intermediate shear stress (Fig. 8) [94]. Current limitation arise from the complex data processing and long computation time which could be solved by further automation and the use of higher processing power.

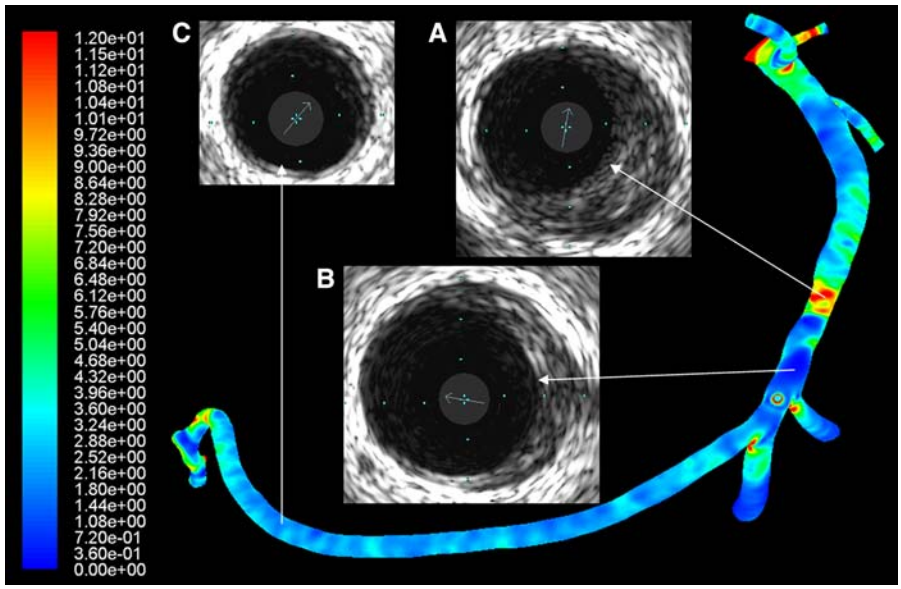

Fig. 8 Color encoded visualization of the wall shear stress as calculated by CFD in a right coronary artery. The 3D model was obtained by MSCT. *Dark blue* areas are exposed to low, *red areas* to high shear stress which is shown by the scheme on the *left*. The small pictures (**a**–**c**) show cross sectional IVUS images of the vessel. In the area of high shear stress a large plaque is shown, which causes an obstruction of the vessel lumen (**a**). The region with low shear stress also shows a high plaque burden, but no narrowing of the lumen can be observed (**b**). In the area with an intermediate level of shear stress the vessel wall remains normal (**c**)

Conclusion

During the last decade the technology in medical imaging has made a substantial progress. Applying modern image reconstruction analysis C-Arm angiography is now able to supply 3-dimensional datasets that can be displayed as either tomographic images or as 3D models. Being comparable to conventional CT for special procedures this new technique of cardiac C-Arm CT is available inside the cath lab without any patient transfer. IVUS as well as OCT, deliver an unsurpassed spatial resolution and will allow for a detailed analysis during intervention. Improvements in automation of signal processing and characterization of more tissue components as well as angiographic integration allow improved guidance in complex interventional procedures which require an optimal spatial orientation. Post processing like CFD analysis of functional parameters is promising to further increase our understanding in plaque progression and maybe in the future allows an earlier treatment of danger prone lesions. However, clinical trials are needed to prove the expected additional benefit for the patient and the physicians.

References

1. Lloyd-Jones D, Adams R, Carnethon M, De Simone G, Ferguson TB, Flegal K et al (2009) Heart disease and stroke statistics—2009 update. A Report From the American Heart Association Statistics Committee and Stroke Statistics Subcommittee. Circulation 119(3):e21–e181
2. Rosamond W, Flegal K, Furie K, Go A, Greenlund K, Haase N et al (2008) Heart disease and stroke statistics—2008 update: a report from the American Heart Association Statistics Committee and Stroke Statistics Subcommittee. Circulation 117:e25–e146. doi:10.1161/CIRCULATIONAHA.107.187998
3. Yusuf S, Reddy S, Ounpuu S, Anand S (2001) Global burden of cardiovascular diseases: part I: general considerations, the epidemiologic transition, risk factors, and impact of urbanization. Circulation 104:2746–2753. doi:10.1161/hc4601.099487
4. Zarocostas J (2008) Three quarters of deaths in developing world will be caused by heart, lung diseases by 2030. BMJ 337:a2322. doi:10.1136/bmj.a2322
5. Mack MJ, Brown PP, Kugelmass AD, Battaglia SL, Tarkington LG, Simon AW et al (2004) Current status and outcomes of coronary revascularization 1999 to 2002: 148, 396 surgical and percutaneous procedures. Ann Thorac Surg 77(3):761–766. doi:10.1016/j.athoracsur.2003.06.019
6. Lauritsch G, Boese J, Wigstrom L, Kemeth H, Fahrig R (2006) Towards cardiac C-arm computed tomography. IEEE Trans Med Imaging 25(7):922–934. doi:10.1109/TMI.2006.876166

7. Bonow RO, Carabello BA, Kanu C, de Leon AC Jr, Faxon DP, Freed MD et al (2006) ACC/AHA 2006 guidelines for the management of patients with valvular heart disease: a report of the American College of Cardiology/American Heart Association Task Force on Practice Guidelines (writing committee to revise the 1998 Guidelines for the Management of Patients With Valvular Heart Disease): developed in collaboration with the Society of Cardiovascular Anesthesiologists: endorsed by the Society for Cardiovascular Angiography and Interventions and the Society of Thoracic Surgeons. Circulation 114(5):e84–e231. doi:10.1161/CIRCULATIONAHA.106.176857
8. Krasemann T (2008) Catheter interventions for congenital heart disease. Herz 33(8):592–600. doi:10.1007/s00059-008-3133-1
9. Patel HT, Hijazi ZM (2005) Pediatric catheter interventions: a year in review 2004–2005. Curr Opin Pediatr 17(5):568–573. doi:10.1097/01.mop.0000172813.56766.52
10. d'Avila A, Ruskin JN (2008) Nonpharmacologic strategies: the evolving story of ablation and hybrid therapy. Am J Cardiol 102(6A):20H–24H. doi:10.1016/j.amjcard.2008.06.026
11. Miller DL (2008) Overview of contemporary interventional fluoroscopy procedures. Health Phys 95(5):638–644. doi:10.1097/01.HP.0000326341.86359.0b
12. Saint-Felix D, Trousset Y, Picard C, Ponchut C, Romeas R, Rougee A (1994) In vivo evaluation of a new system for 3D computerized angiography. Phys Med Biol 39(3):583–595. doi:10.1088/0031-9155/39/3/020
13. Fahrig R, Fox AJ, Lownie S, Holdsworth DW (1997) Use of a C-arm system to generate true three-dimensional computed rotational angiograms: preliminary in vitro and in vivo results. AJNR Am J Neuroradiol 18(8):1507–1514
14. Jaffray DA, Siewerdsen JH (2000) Cone-beam computed tomography with a flat-panel imager: initial performance characterization. Med Phys 27(6):1311–1323. doi:10.1118/1.599009
15. Groh BA, Siewerdsen JH, Drake DG, Wong JW, Jaffray DA (2002) A performance comparison of flat-panel imager-based MV and kV cone-beam CT. Med Phys 29(6):967–975. doi:10.1118/1.1477234
16. Ritter D, Orman J, Schmidgunst C, Graumann R (2007) 3D soft tissue imaging with a mobile C-arm. Comput Med Imaging Graph 31(2):91–102. doi:10.1016/j.compmedimag.2006.11.003
17. Kalender WA, Kyriakou Y (2007) Flat-detector computed tomography (FD-CT). Eur Radiol 17(11):2767–2779. doi:10.1007/s00330-007-0651-9
18. Feldkamp LA, Davis LC, Webb S (1988) Comments, with reply, on;Tomographic reconstruction from experimentally obtained cone-beam projections' by S Webb, et al. IEEE Trans Med Imaging 7(1):73–74. doi:10.1109/42.3930
19. Reiser MF, Becker CR, Nikolaou K, Glazer G (2009) Multislice CT, 3rd edn. Springer, Heidelberg
20. Fuster V, Ryden LE, Cannom DS, Crijns HJ, Curtis AB, Ellenbogen KA et al (2006) ACC/AHA/ESC 2006 guidelines for the management of patients with atrial fibrillation: full text: a report of the American College of Cardiology/American Heart Association Task Force on practice guidelines and the European Society of Cardiology Committee for Practice Guidelines (Writing Committee to Revise the 2001 guidelines for the management of patients with atrial fibrillation) developed in collaboration with the European Heart Rhythm Association and the Heart Rhythm Society. Europace 8(9):651–745. doi:10.1093/europace/eul097
21. Callahan TD, Di Biase L, Horton R, Sanchez J, Gallinghouse JG, Natale A (2009) Catheter ablation of atrial fibrillation. Cardiol Clin 27(1):163–178. doi:10.1016/j.ccl.2008.09.004
22. Khan MN, Jais P, Cummings J, Di Biase L, Sanders P, Martin DO et al (2008) Pulmonary-vein isolation for atrial fibrillation in patients with heart failure. N Engl J Med 359(17):1778–1785. doi:10.1056/NEJMoa0708234
23. Lakkireddy D, Nadzam G, Verma A, Prasad S, Ryschon K, Di Biase L et al (2009) Impact of a comprehensive safety program on radiation exposure during catheter ablation of atrial fibrillation: a prospective study. J Interv Card Electrophysiol 24(2):105–112
24. Takahashi A, Kuwahara T, Takahashi Y (2009) Complications in the Catheter Ablation of Atrial Fibrillation. Circ J 73(2):221–226
25. Nolker G, Gutleben KJ, Marschang H, Ritscher G, Asbach S, Marrouche N et al (2008) Three-dimensional left atrial and esophagus reconstruction using cardiac C-arm computed tomography with image integration into fluoroscopic views for ablation of atrial fibrillation: accuracy of a novel modality in comparison with multislice computed tomography. Heart Rhythm 5(12):1651–1657. doi:10.1016/j.hrthm.2008.09.011
26. Rohkohl C, Lauritsch G, Nöttling A, Prümmer M, Hornegger (2008) J C-Arm CT: Reconstruction of dynamic high contrast objects applied to the coronary sinus. Conference Record of the 2008 IEEE Nuclear Science Symposium, Oct 19–25. Dresden, Germany, pp 5113–5120
27. Prümmer M, Wigstroem L, Hornegger J, Boese J, Lauritsch G, Strobel N, Fahrig R (2006) Cardiac c-arm CT: efficient motion correction for 4d-fbp. Conference Record of the 2006 IEEE Nuclear Science Symposium, Oct 29–Nov 4. San Diego, CA, USA, pp 2620–2628
28. Albouaini K, Egred M, Rao A, Alahmar A, Wright DJ (2008) Cardiac resynchronisation therapy: evidence based benefits and patient selection. Eur J Intern Med 19(3):165–172. doi:10.1016/j.ejim.2007.09.012
29. Kerwin WF, Paz O (2003) Cardiac resynchronization therapy: overcoming ventricular dyssynchrony in dilated heart failure. Cardiol Rev 11(4):221–239. doi:10.1097/01.CRD.0000078444.96998.99
30. Dickstein K, Cohen-Solal A, Filippatos G, McMurray JJ, Ponikowski P, Poole-Wilson PA et al (2008) ESC Guidelines for the diagnosis and treatment of acute and chronic heart failure 2008: the Task Force for the Diagnosis and Treatment of Acute and Chronic Heart Failure 2008 of the European Society of Cardiology. Developed in collaboration with the Heart Failure Association of the ESC (HFA) and endorsed by the European Society of Intensive Care Medicine (ESICM). Eur Heart J 29(19):2388–2442. doi:10.1093/eurheartj/ehn309
31. Burkhardt JD, Wilkoff BL (2007) Interventional electrophysiology and cardiac resynchronization therapy: delivering electrical therapies for heart failure. Circulation 115(16):2208–2220. doi:10.1161/CIRCULATIONAHA.106.655712

32. Frattini F, Rordorf R, Angoli L, Pentimalli F, Vicentini A, Petracci B et al (2008) Left ventricular pacing lead positioning in the target vein of the coronary sinus: description of a challenging case. Pacing Clin Electrophysiol 31(4):503–505. doi:10.1111/j.1540-8159.2008.01022.x
33. Alfieri O, Maisano F, Colombo A (2005) Future of transcatheter repair of the mitral valve. Am J Cardiol 96(12A): 71L–75L. doi:10.1016/j.amjcard.2005.09.065
34. Feldman T (2007) Percutaneous mitral valve repair. J Interv Cardiol 20(6):488–494. doi:10.1111/j.1540-8183.2007.00295.x
35. Knuuti J, Bengel FM (2008) Positron emission tomography and molecular imaging. Heart 94(3):360–367. doi:10.1136/hrt.2007.118992
36. Reddy GP, Pujadas S, Ordovas KG, Higgins CB (2008) MR imaging of ischemic heart disease. Magn Reson Imaging Clin N Am 16(2):201–212. doi:10.1016/j.mric.2008.03.002
37. Baks T, Cademartiri F, Moelker AD, Weustink AC, van Geuns RJ, Mollet NR et al (2006) Multislice computed tomography and magnetic resonance imaging for the assessment of reperfused acute myocardial infarction. J Am Coll Cardiol 48(1):144–152. doi:10.1016/j.jacc.2006.02.059
38. Koyama Y, Mochizuki T, Higaki J (2004) Computed tomography assessment of myocardial perfusion, viability, and function. J Magn Reson Imaging 19(6):800–815. doi:10.1002/jmri.20067
39. Ruzsics B, Lee H, Powers ER, Flohr TG, Costello P, Schoepf UJ (2008) Images in cardiovascular medicine. Myocardial ischemia diagnosed by dual-energy computed tomography: correlation with single-photon emission computed tomography. Circulation 117(9):1244–1245. doi:10.1161/CIRCULATIONAHA.107.745711
40. Schoenhagen P, Nissen S (2002) Understanding coronary artery disease: tomographic imaging with intravascular ultrasound. Heart 88(1):91–96. doi:10.1136/heart.88.1.91
41. Regar E, Werner F, Klauss V, Siebert U, Henneke KH, Rieber J et al (1999) IVUS analysis of the acute and long-term stent result using motorized pullback: intraobserver and interobserver variability. Catheter Cardiovasc Interv 48(3):245–250. doi:10.1002/(SICI)1522-726X(199911)48:3<245:AID-CCD1>3.0.CO;2-9
42. Regar E, Werner F, Siebert U, Rieber J, Theisen K, Mudra H et al (2000) Reproducibility of neointima quantification with motorized intravascular ultrasound pullback in stented coronary arteries. Am Heart J 139(4):632–637. doi:10.1016/S0002-8703(00)90040-1
43. Schroeder AP, Falk E (1995) Vulnerable and dangerous coronary plaques. Atherosclerosis 118(Suppl):S141–S149
44. Ross R (1999) Atherosclerosis–an inflammatory disease. N Engl J Med 340(2):115–126. doi:10.1056/NEJM199901143400207
45. Schaar JA, Muller JE, Falk E, Virmani R, Fuster V, Serruys PW et al (2004) Terminology for high-risk, vulnerable coronary artery plaques. Report of a meeting on the vulnerable plaque, June 17, 18, 2003, Santorini, Greece. Eur Heart J 25(12):1077–1082. doi:10.1016/j.ehj.2004.01.002
46. Hirose M, Kobayashi Y, Mintz GS, Moussa I, Mehran R, Lansky AJ et al (2003) Correlation of coronary arterial remodeling determined by intravascular ultrasound with angiographic diameter reduction of 20% to 60%. Am J Cardiol 92(2):141–145. doi:10.1016/S0002-9149(03)00528-9
47. Schoenhagen P, Nissen SE, Tuzcu EM (2003) Coronary arterial remodeling: from bench to bedside. Curr Atheroscler Rep 5(2):150–154. doi:10.1007/s11883-003-0088-9
48. Siegel RJ, Ariani M, Fishbein MC, Chae JS, Park JC, Maurer G et al (1991) Histopathologic validation of angioscopy and intravascular ultrasound. Circulation 84(1): 109–117
49. Leber AW, Knez A, Becker A, Becker C, von Ziegler F, Nikolaou K et al (2004) Accuracy of multidetector spiral computed tomography in identifying and differentiating the composition of coronary atherosclerotic plaques: a comparative study with intracoronary ultrasound. J Am Coll Cardiol 43(7):1241–1247. doi:10.1016/j.jacc.2003.10.059
50. Ge J, Erbel R, Gerber T, Gorge G, Koch L, Haude M et al (1994) Intravascular ultrasound imaging of angiographically normal coronary arteries: a prospective study in vivo. Br Heart J 71(6):572–578. doi:10.1136/hrt.71.6.572
51. Peters RJ, Kok WE, Havenith MG, Rijsterborgh H, van der Wal AC, Visser CA (1994) Histopathologic validation of intracoronary ultrasound imaging. J Am Soc Echocardiogr 7(3 Pt 1):230–241
52. Wilson LS, Neale ML, Talhami HE, Appleberg M (1994) Preliminary results from attenuation-slope mapping of plaque using intravascular ultrasound. Ultrasound Med Biol 20(6):529–542. doi:10.1016/0301-5629(94)90089-2
53. Lizzi FL, Greenebaum M, Feleppa EJ, Elbaum M, Coleman DJ (1983) Theoretical framework for spectrum analysis in ultrasonic tissue characterization. J Acoust Soc Am 73(4):1366–1373. doi:10.1121/1.389241
54. Moore MP, Spencer T, Salter DM, Kearney PP, Shaw TR, Starkey IR et al (1998) Characterisation of coronary atherosclerotic morphology by spectral analysis of radiofrequency signal: in vitro intravascular ultrasound study with histological and radiological validation. Heart 79(5): 459–467
55. Konig A, Klauss V (2007) Virtual histology. Heart 93(8):977–982. doi:10.1136/hrt.2007.116384
56. Nair A, Kuban BD, Tuzcu EM, Schoenhagen P, Nissen SE, Vince DG (2002) Coronary plaque classification with intravascular ultrasound radiofrequency data analysis. Circulation 106(17):2200–2206. doi:10.1161/01.CIR.0000035654.18341.5E
57. Rodriguez-Granillo GA, McFadden EP, Valgimigli M, van Mieghem CA, Regar E, de Feyter PJ et al (2006) Coronary plaque composition of nonculprit lesions, assessed by in vivo intracoronary ultrasound radio frequency data analysis, is related to clinical presentation. Am Heart J 151(5):1020–1024. doi:10.1016/j.ahj.2005.06.040
58. Huang D, Swanson EA, Lin CP, Schuman JS, Stinson WG, Chang W et al (1991) Optical coherence tomography. Science 254(5035):1178–1181. doi:10.1126/science.1957169
59. Brezinski ME, Tearney GJ, Bouma BE, Boppart SA, Hee MR, Swanson EA et al (1996) Imaging of coronary artery microstructure (in vitro) with optical coherence tomography. Am J Cardiol 77(1):92–93. doi:10.1016/S0002-9149(97)89143-6

60. Hee MR, Izatt JA, Swanson EA, Huang D, Schuman JS, Lin CP et al (1995) Optical coherence tomography of the human retina. Arch Ophthalmol 113(3):325–332
61. Tearney GJ, Brezinski ME, Bouma BE, Boppart SA, Pitris C, Southern JF et al (1997) In vivo endoscopic optical biopsy with optical coherence tomography. Science 276(5321):2037–2039. doi:10.1126/science.276.5321.2037
62. Jang IK, Bouma BE, Kang DH, Park SJ, Park SW, Seung KB et al (2002) Visualization of coronary atherosclerotic plaques in patients using optical coherence tomography: comparison with intravascular ultrasound. J Am Coll Cardiol 39(4):604–609. doi:10.1016/S0735-1097(01)01799-5
63. Jang IK, Tearney GJ, MacNeill B, Takano M, Moselewski F, Iftima N et al (2005) In vivo characterization of coronary atherosclerotic plaque by use of optical coherence tomography. Circulation 111(12):1551–1555. doi:10.1161/01.CIR.0000159354.43778.69
64. Liu B, Brezinski ME (2007) Theoretical and practical considerations on detection performance of time domain, Fourier domain, and swept source optical coherence tomography. J Biomed Opt 12(4):044007. doi:10.1117/1.2753410
65. Yun SH (2006) Optical coherence tomography using rapidly swept lasers. Conf Proc IEEE Eng Med Biol Soc 1:125–128. doi:10.1109/IEMBS.2006.260859
66. Low AF, Tearney GJ, Bouma BE, Jang IK (2006) Technology Insight: optical coherence tomography—current status and future development. Nat Clin Pract Cardiovasc Med 3(3):154–162. doi:10.1038/ncpcardio0482
67. Pinto TL, Waksman R (2006) Clinical applications of optical coherence tomography. J Interv Cardiol 19(6):566–573. doi:10.1111/j.1540-8183.2006.00201.x
68. Guagliumi G, Sirbu V (2008) Optical coherence tomography: high resolution intravascular imaging to evaluate vascular healing after coronary stenting. Catheter Cardiovasc Interv 72(2):237–247. doi:10.1002/ccd.21606
69. Fujimoto JG, Boppart SA, Tearney GJ, Bouma BE, Pitris C, Brezinski ME (1999) High resolution in vivo intra-arterial imaging with optical coherence tomography. Heart 82(2):128–133
70. Brezinski ME, Tearney GJ, Bouma BE, Izatt JA, Hee MR, Swanson EA et al (1996) Optical coherence tomography for optical biopsy. Properties and demonstration of vascular pathology. Circulation 93(6):1206–1213
71. Yabushita H, Bouma BE, Houser SL, Aretz HT, Jang IK, Schlendorf KH et al (2002) Characterization of human atherosclerosis by optical coherence tomography. Circulation 106(13):1640–1645. doi:10.1161/01.CIR.0000029927.92825.F6
72. Meissner OA, Rieber J, Babaryka G, Oswald M, Reim S, Siebert U et al (2006) Intravascular optical coherence tomography: comparison with histopathology in atherosclerotic peripheral artery specimens. J Vasc Interv Radiol 17(2 Pt 1):343–349
73. Rieber J, Meissner O, Babaryka G, Reim S, Oswald M, Koenig A et al (2006) Diagnostic accuracy of optical coherence tomography and intravascular ultrasound for the detection and characterization of atherosclerotic plaque composition in ex-vivo coronary specimens: a comparison with histology. Coron Artery Dis 17(5):425–430. doi:10.1097/00019501-200608000-00005
74. Nemirovsky D (2003) Imaging of high-risk plaque. Cardiology 100(4):160–175. doi:10.1159/000074810
75. Tearney GJ, Yabushita H, Houser SL, Aretz HT, Jang IK, Schlendorf KH et al (2003) Quantification of macrophage content in atherosclerotic plaques by optical coherence tomography. Circulation 107(1):113–119. doi:10.1161/01.CIR.0000044384.41037.43
76. Virmani R, Kolodgie FD, Burke AP, Farb A, Schwartz SM (2000) Lessons from sudden coronary death: a comprehensive morphological classification scheme for atherosclerotic lesions. Arterioscler Thromb Vasc Biol 20(5):1262–1275
77. MacNeill BD, Lowe HC, Takano M, Fuster V, Jang IK (2003) Intravascular modalities for detection of vulnerable plaque: current status. Arterioscler Thromb Vasc Biol 23(8):1333–1342. doi:10.1161/01.ATV.0000080948.08888.BF
78. Takano M, Inami S, Jang IK, Yamamoto M, Murakami D, Seimiya K et al (2007) Evaluation by optical coherence tomography of neointimal coverage of sirolimus-eluting stent three months after implantation. Am J Cardiol 99(8):1033–1038. doi:10.1016/j.amjcard.2006.11.068
79. Diaz-Sandoval LJ, Bouma BE, Tearney GJ, Jang IK (2005) Optical coherence tomography as a tool for percutaneous coronary interventions. Catheter Cardiovasc Interv 65(4):492–496. doi:10.1002/ccd.20340
80. Bouma BE, Tearney GJ, Yabushita H, Shishkov M, Kauffman CR, DeJoseph GD et al (2003) Evaluation of intracoronary stenting by intravascular optical coherence tomography. Heart 89(3):317–320. doi:10.1136/heart.89.3.317
81. Giattina SD, Courtney BK, Herz PR, Harman M, Shortkroff S, Stamper DL et al (2006) Assessment of coronary plaque collagen with polarization sensitive optical coherence tomography (PS-OCT). Int J Cardiol 107(3):400–409. doi:10.1016/j.ijcard.2005.11.036
82. Bazant-Hegemark F, Stone N (2009) Towards automated classification of clinical optical coherence tomography data of dense tissues. Lasers Med Sci 24(4):627–638
83. Boppart SA, Oldenburg AL, Xu C, Marks DL (2005) Optical probes and techniques for molecular contrast enhancement in coherence imaging. J Biomed Opt 10(4):41208. doi:10.1117/1.2008974
84. Zysk AM, Nguyen FT, Oldenburg AL, Marks DL, Boppart SA (2007) Optical coherence tomography: a review of clinical development from bench to bedside. J Biomed Opt 12(5):051403. doi:10.1117/1.2793736
85. Gimbrone MA Jr (1999) Endothelial dysfunction, hemodynamic forces, and atherosclerosis. Thromb Haemost 82(2):722–726
86. Malek AM, Alper SL, Izumo S (1999) Hemodynamic shear stress and its role in atherosclerosis. JAMA 282(21):2035–2042. doi:10.1001/jama.282.21.2035
87. Frangos SG, Gahtan V, Sumpio B (1999) Localization of atherosclerosis: role of hemodynamics. Arch Surg 134(10):1142–1149. doi:10.1001/archsurg.134.10.1142
88. Frauenfelder T, Boutsianis E, Schertler T, Husmann L, Leschka S, Poulikakos D et al (2007) In vivo flow simulation in coronary arteries based on computed tomography datasets: feasibility and initial results. Eur Radiol 17(5):1291–1300. doi:10.1007/s00330-006-0465-1

89. Boutsianis E, Dave H, Frauenfelder T, Poulikakos D, Wildermuth S, Turina M et al (2004) Computational simulation of intracoronary flow based on real coronary geometry. Eur J Cardiothorac Surg 26(2):248–256. doi:10.1016/j.ejcts.2004.02.041
90. Sankaranarayanan M, Chua LP, Ghista DN, Tan YS (2006) Flow studies in three-dimensional aorto-right coronary bypass graft system. J Med Eng Technol 30(5):269–282. doi:10.1080/03091900500217281
91. Goubergrits L, Kertzscher U, Schoneberg B, Wellnhofer E, Petz C, Hege HC (2008) CFD analysis in an anatomically realistic coronary artery model based on non-invasive 3D imaging: comparison of magnetic resonance imaging with computed tomography. Int J Cardiovasc Imaging 24(4): 411–421. doi:10.1007/s10554-007-9275-z
92. Radaelli AG, Augsburger L, Cebral JR, Ohta M, Rufenacht DA, Balossino R et al (2008) Reproducibility of haemodynamical simulations in a subject-specific stented aneurysm model—a report on the virtual intracranial stenting challenge 2007. J Biomech 41(10):2069–2081. doi:10.1016/j.jbiomech.2008.04.035
93. LaDisa JF Jr, Olson LE, Douglas HA, Warltier DC, Kersten JR, Pagel PS (2006) Alterations in regional vascular geometry produced by theoretical stent implantation influence distributions of wall shear stress: analysis of a curved coronary artery using 3D computational fluid dynamics modeling. Biomed Eng Online 5:40. doi:10.1186/1475-925X-5-40
94. Rieber J, Redel T, Hetterich H, Potzger T, Nikolaou K, Rist C, Klauss V (2008) Abstract 2800: assessment of computational fluid dynamics to calculate individual coronary wall shear stress in vivo. Circulation 118(S_777-b)